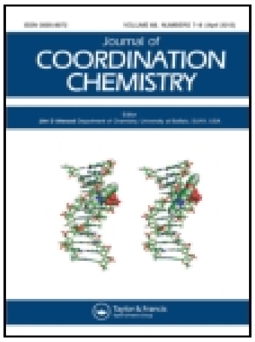

Journal of
COORDINATION
CHEMISTRY

Taylor & Francis
Taylor & Francis Group

Journal of Coordination Chemistry

ISSN: 0095-8972 (Print) 1029-0389 (Online) Journal homepage: http://www.tandfonline.com/loi/gcoo20

Syntheses and crystal structures of four lanthanide complexes based on two tri-protonated hexacarboxylic acids of 1,2,3,4,5,6-cyclohexane-hexacarboxylic acid and mellitic acid

Hongzhen Xie & Guanzhong Lu

To cite this article: Hongzhen Xie & Guanzhong Lu (2015) Syntheses and crystal structures of four lanthanide complexes based on two tri-protonated hexacarboxylic acids of 1,2,3,4,5,6-cyclohexane-hexacarboxylic acid and mellitic acid, Journal of Coordination Chemistry, 68:10, 1800-1813, DOI: 10.1080/00958972.2015.1023717

To link to this article: http://dx.doi.org/10.1080/00958972.2015.1023717

Journal of Coordination Chemistry, 2015
Vol. 68, No. 10, 1800–1813, http://dx.doi.org/10.1080/00958972.2015.1023717

Syntheses and crystal structures of four lanthanide complexes based on two tri-protonated hexacarboxylic acids of 1,2,3,4,5,6-cyclohexane-hexacarboxylic acid and mellitic acid

HONGZHEN XIE†‡ and GUANZHONG LU*†

†Key Laboratory for Advanced Materials and Research Institute of Industrial Catalysis, East China University of Science and Technology, Shanghai, PR China
‡State Key Laboratory Base of Novel Functional Materials and Preparation Science, Faculty of Materials Science and Chemical Engineering, Ningbo University, Ningbo, PR China

(*Received 8 April 2014; accepted 2 February 2015*)

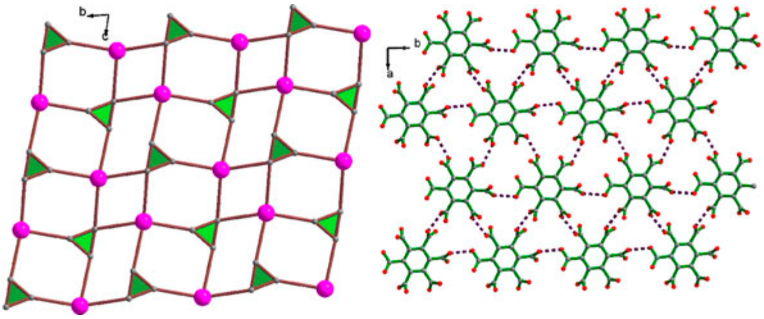

Four lanthanide complexes with two tri-protonated hexacarboxylic acids [1,2,3,4,5,6-cyclohexane-hexacarboxylic acid (H_6chhc) and mellitic acid (H_6Mel)], [Pr(H_3chhc)(DMF)$_3$(H_2O)]·H_2O (**1**), Nd(H_3chhc)(DMF)$_3$ (**2**), [Er(H_2O)$_8$]·(H_3Mel)·9(H_2O) (**3**), and [Yb(H_2O)$_8$]·(H_3Mel)·8.5(H_2O) (**4**), have been synthesized in solution at room temperature and characterized by elemental analysis, IR spectrum, and single-crystal X-ray diffraction. The crystal structures of **1** and **2** are made up of a (4^4, 6^2) 2-D network extended infinitely parallel to the (1 0 0) plane. The H_3chhc^{3-} anions assume a *cis-e,a, e,a,e,a*-conformation with the central ring in chair-shaped configuration. In **3** and **4**, the H_3Mel^{3-} as counter ions are interconnected by hydrogen bonds to form 2-D organic supramolecular layers. The coordination modes and abilities of H_6chhc and mellitic acid are discussed and compared. The luminescences of **1**–**4** have been investigated.

Keywords: Lanthanide complexes; Crystal structures; 1,2,3,4,5,6-Cyclohexane-hexacarboxylic acid; Mellitic acid; Synthesis

1. Introduction

Crystal engineering of lanthanide complexes has attracted attention because of their intriguing topological structures and potential applications [1–5]. Lanthanide ions with high

---

*Corresponding author. Email: gzhlu@ecust.edu.cn coordination numbers and variable coordination environments combining with ligands can be assembled into lanthanide coordination frameworks with unusual structures [6, 7]. Polycarboxylate ligands have been extensively used as organic spacers for construction of coordination frameworks. There are two types of important ligands, benzene-based and flexible polycarboxylates [8–11], in which hexacarboxylic acids with six carboxylic groups, such as 1,2,3,4,5,6-cyclohexane-hexacarboxylic (H_6chhc) acid and mellitic acid, are also used to synthesize lanthanide coordination frameworks [12, 13]. H_6chhc and mellitic acid have similarities and differences; both have a six-membered ring and six carboxyl groups with 12 potential donors and display outstanding denticity and assembling power. The differences are mellitic acid with a rigid six-membered aromatic ring is often used as building block to construct porous MOFs and to synthesise lanthanide luminescence materials due to no hydrogen thermal vibration [14] and the six-membered ring of H_6chhc possesses diverse conformations based on its single-bonded cyclo skeleton in combination with equatorial or axial orientations of the carboxyl groups, leading to abundant coordination behaviors.

In these lanthanide coordination frameworks, most forms are the deprotonated hexacarboxylic acids, chhc^{6-} and mel^{6-}, respectively, and these complexes are mostly obtained in hydrothermal conditions [15, 16]. However, the various protonated forms of the two hexacarboxylic acids in lanthanide complexes are barely reported [17, 18]. The deprotonation degree of six carboxyl groups in H_6chhc could affect the topology and dimensionality of lanthanide coordination frameworks [13]. Commercial H_6chhc is the all-*cis* (*a*,*e*,*a*,*e*,*a*,*e*) with chair comformations, which often undergoes isomerization during metal complexation under hydrothermal conditions. For example, Tong and coworkers obtained various isomers of H_6chhc in coordination complexes, but they are mostly *trans* (*e,e,e,e,e,e*) isomers [19–21]. In these complexes, the initial transformations of all-*cis* H_6chhc with the carboxylic groups alternately in equatorial and axial positions have transformed into all-*trans* with all groups in the equatorial positions.

To compare the coordination chemistry of the two hexacarboxylic acids, explore the effect of deprotonation degree on the topology and dimensionality of lanthanide coordination framework, investigate an approach to avoid the transformations of H_6chhc ligands into other isomers, and obtain new lanthanide–mellitic acid complexes in mild solution conditions; we have synthesized four lanthanide complexes in solution at room temperature with tri-protonated hexacarboxylic acid: $[Pr(H_3chhc)(DMF)_3(H_2O)]\cdot H_2O$ (**1**), $Nd(H_3chhc)(DMF)_3$ (**2**), $Ln(H_2O)_8\cdot(H_3Mel)\cdot 9(H_2O)$ (**3**), and $[Yb(H_2O)_8]\cdot(H_3Mel)\cdot 8.5(H_2O)$ (**4**).

2. Experimental

2.1. *Preparation of 1–4*

$Er(NO_3)_3\cdot nH_2O$ and $Yb(NO_3)_3\cdot nH_2O$ were prepared in our laboratory. Other chemicals of reagent grade were commercially available (Aladdin) and used without purification.

2.1.1. Synthesis of $[Pr(H_3chhc)(DMF)_3(H_2O)]\cdot H_2O$ (1). *All-cis*-1,2,3,4,5,6-cyclohexanehexacarboxylic acid (H_6chhc) 0.175 g (0.5 mmol) was dissolved in water (5 mL) and DMF (5 mL). 0.217 g (0.5 mmol) $Pr(NO_3)_3\cdot 6H_2O$ was added to the above solution under stirring. The formed pale green solution was kept at room temperature for slow evaporation of solvent. Green flaky crystals were obtained after one week (yield: 0.123 g, 34% based on initial $Pr(NO_3)_3{\cdot}6H_2O$). IR (Infrared spectra, KBr pellet, cm^{-1}): 3425(s), 1705(s), 1603(s), 1564(vs), 1376(m), 1208(m), 1170(s), 1042(m), 918(m), 880(s), 804(w), 765(s), 717(m), 638(w). Anal. Calcd. for $C_{21}H_{34}N_3PrO_{17}$ (%): C, 34.01; H, 4.63; N, 5.67. Found: C, 34.21; H, 4.56; N, 5.72.

2.1.2. Synthesis of $Nd(H_3chhc)(DMF)_3$ (2). Purple crystals were prepared analogously to **1** except using $Nd(NO_3)_3{\cdot}6H_2O$ 0.219 g (0.5 mmol) instead of $Pr(NO_3)_3{\cdot}6H_2O$ (Yield: 0.043 g, 12% based on initial $Nd(NO_3)_3{\cdot}nH_2O$). IR (Infrared spectra, KBr pellet, cm^{-1}): 3439(w), 2994(w), 1713(s), 1606(vs), 1569(vs), 1385(s), 1319(m), 1219(s), 1180(s), 1076 (s), 1035(m), 1011(m), 929(s), 873(m), 816(m), 768(s), 728(s), 638(s). Anal. Calcd for $C_{21}H_{30}N_3NdO_{15}$ (%): C, 35.59; H, 4.28; N, 5.93. Found: C, 35.53; H, 4.31; N, 5.87.

2.1.3. Synthesis of $Er(H_2O)_8{\cdot}(H_3Mel){\cdot}9(H_2O)$ (3). $Er(NO_3)_3{\cdot}nH_2O$ was obtained by slow evaporation of a solution of 0.0382 g (0.1 mmol) Er_2O_3 dissolved in HNO_3 under water boiling condition. The resulting $Er(NO_3)_3{\cdot}nH_2O$ and mellitic acid 0.0700 g (0.2 mmol) were stirred in H_2O (10 mL) at room temperature. The resulting solution was kept at room temperature and afforded pink block crystals of $[Er(H_2O)_8]{\cdot}(H_3Mel){\cdot}9(H_2O)$ (**3**) after several days (Yield: 0.114 g, 70% based on initial Er_2O_3). IR (Infrared spectra, KBr pellet, cm^{-1}): 3420(s), 1615(s), 1435(s), 1343(m), 1279(m), 876(m), 722(w), 623(m), 485(w). Anal. Calcd for $C_{12}H_{37}ErO_{29}$ (%): C, 17.73; H, 4.60. Found: C, 17.59; H, 4.45.

2.1.4. Synthesis of $[Yb(H_2O)_8]{\cdot}(H_3Mel){\cdot}8.5(H_2O)$ (4). $Yb(NO_3)_3{\cdot}nH_2O$ was obtained by the same method as $Er(NO_3)_3{\cdot}nH_2O$. The synthesis of $Yb(H_2O)_8{\cdot}(H_3Mel){\cdot}8.5(H_2O)$ (**4**) is similar to **3**, only $Yb(NO_3)_3{\cdot}nH_2O$ substituted for $Er(NO_3)_3{\cdot}nH_2O$. (Yield: 0.097 g, 60% based on initial Yb_2O_3). IR (KBr pellet, cm^{-1}): 3426(s), 1628(s), 1463(s), 1345(m), 1285 (m), 868(m), 726(m), 633(m), 465(w). Anal. Calcd for $C_{12}H_{36}YbO_{28.5}$ (%): C, 17.80; H, 4.49. Found: C, 17.67; H, 4.48.

2.2. *Analytic methods of samples*

FT-IR spectra of samples were recorded on a Shimadzu FT-IR-8900 spectrometer, and the sample to be measured was ground with KBr and pressed into a thin wafer. Elemental analyses of C, H, and N were performed on a Perkin Elmer 2400II CHNS/O full automatic analyzer. Powder X-ray diffraction (PXRD) was performed on a Bruker D8 Advance diffractometer with CuKα radiation ($\lambda = 1.5406$ Å). Solid-state powder luminescence spectra of samples were recorded on an F-4600 (Hitachi) fluorescence spectrofluorimeter.

2.3. *Single-crystal X-ray diffraction analysis*

Single crystals of **1–4** were analyzed by single-crystal X-ray diffraction at 298(2)K. Data collections were performed on a RIGAKU RAXIS–RAPID diffractometer with graphite monochromated MoKα radiation ($\lambda = 0.71073$ Å). All calculations were carried out with SHELXTL-97 [22, 23]. The structures were refined by full matrix least squares with anisotropic displacement parameters for non-hydrogen atoms. The hydrogens were generated

Table 1. Crystal data and structure refinements for **1–4**.

Compound	**1**	**2**	**3**	**4**
Formula	$C_{21}H_{34}N_3PrO_{17}$	$C_{21}H_{30}N_3NdO_{15}$	$C_{12}H_{37}ErO_{29}$	$C_{12}H_{36}YbO_{28.5}$
Formula mass	741.42	708.72	812.68	809.45
Crystal system	Triclinic	Monoclinic	Monoclinic	Monoclinic
Space group	*P-1*	$P2_1/c$	$P2_1/c$	$P2_1/c$
a (Å)	10.629(2)	10.968(2)	15.824(2)	15.824(2)
b (Å)	11.146(2)	11.489(2)	9.558(1)	9.558(1)
c (Å)	11.671(2)	21.555(4)	19.473(2)	19.473(2)
α (°)	77.54(3)	90	90	90
β (°)	87.24(3)	101.48(3)	98.751(1)	98.751(1)
γ (°)	85.65(3)	90	90	90
Volume (Å^3)	1345.5(4)	2661.8(8)	2911.0(5)	2911.0(4)
Z	2	4	4	4
D_{Calcd} (g cm^{-3})	1.830	1.768	1.854	1.847
μ (mm^{-1})	1.899	2.030	2.996	3.323
$F(0\,0\,0)$	752	1428	1636	1624
2θ range (°)	3.14–27.40	3.00–25.00	3.08–27.12	3.12–26.82
R_1, wR_2 [$I > 2\sigma(I)$]^a	0.0651, 0.1407	0.0423, 0.0952	0.0305, 0.0838	0.0306, 0.0771
R_1, wR_2 (all data)	0.1075, 0.1947	0.0635, 0.1166	0.0333, 0.0860	0.0337, 0.0789
GOF	1.007	1.109	1.007	1.014

$^a wR_2 = [\Sigma w(F_o^2 - F_c^2)^2/\Sigma w(F_o^2)^2]^{1/2}$.

geometrically and treated as riding or found in the electron density maps but fixed in the riding model. Details of crystal data, collection, and refinement of **1–4** are summarized in table 1.

3. Results and discussion

Through H_6chhc or mellitic acid reacted with $Ln(NO_3)_3\cdot nH_2O$ in solution at room temperature without adjusting pH, two types of compounds with different structures were obtained (scheme 1). The common characteristic of the four complexes is that only three protons have been removed from six carboxyl groups of H_6chhc and mellitic acid. The coordination polymers [Pr(H_3chhc)$(DMF)_3(H_2O)]\cdot H_2O$ (**1**) and Nd(H_3chhc)$(DMF)_3$ (**2**) were obtained in mixed solution of DMF and H_2O because of the poor solubility of H_6chhc in H_2O. H_3chhc^{3-} complexes were mostly synthesized by adjusting pH with NaOH [17, 18] or NH_3 solution [21] and obtained by heating [17] or sol–gel method [18]. $Er(H_2O)_8\cdot(H_3Mel)\cdot 9(H_2O)$ (**3**) and $[Yb(H_2O)_8]\cdot(H_3Mel)\cdot 8.5(H_2O)$ (**4**) were synthesized in aqueous solution at room temperature.

H_3Mel^{3-} form of mellitic acid was rarely reported in complexes. The mellitic acids were fully deprotonated (mel^{6-}) in most lanthanide complexes, which were prepared by the hydrothermal method [12, 16], diffusion method [24, 25], or sol–gel method [26].

3.1. *The crystal structures of [Pr(H_3chhc)$(DMF)_3(H_2O)]\cdot H_2O$ (1) and Nd(H_3chhc)$(DMF)_3$ (2)*

The data from X-ray diffraction crystal structure analysis reveals that **1** is a 2-D framework with crystallization in *P-1* space group. The asymmetric unit is comprised of one Pr(III), one H_3chhc^{3-}, three DMF molecules, one water ligand, and one lattice water [figure 1(a)].

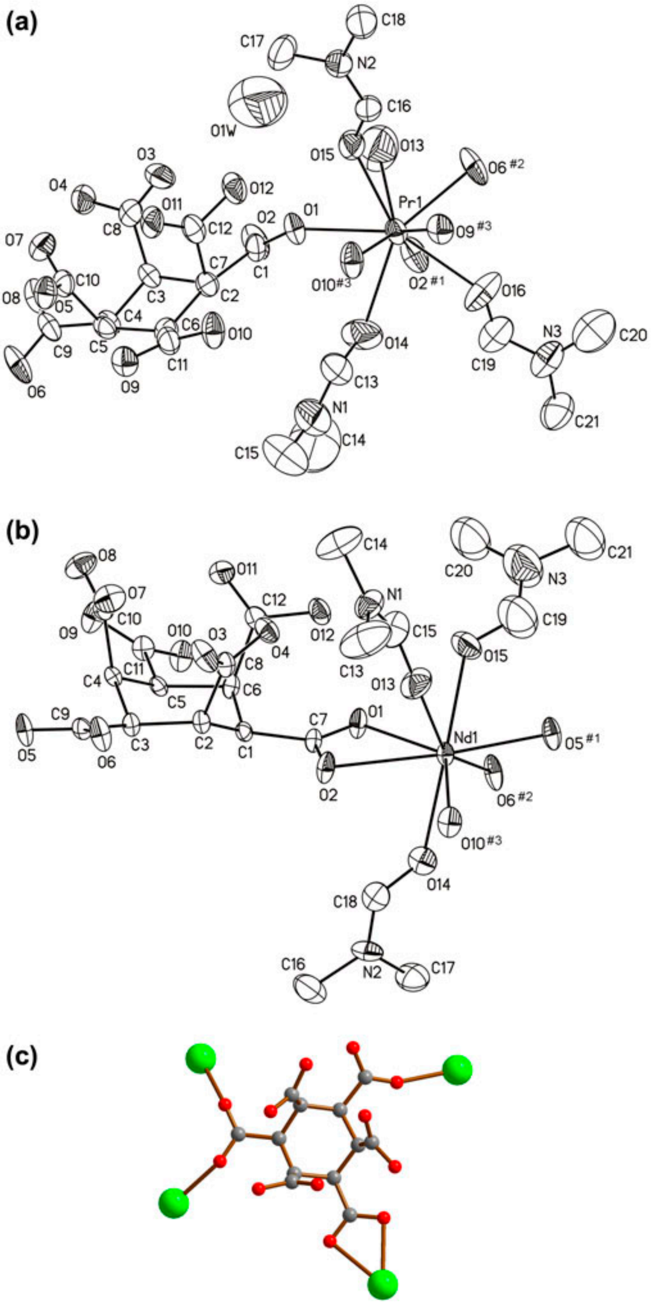

Figure 1. (a) ORTEP view of coordination environment of Pr(III) in **1** along with the atom numbering scheme and thermal ellipsoids drawn at 45% probability (#1 = $-x + 1$, $-y$, $-z + 1$; #2 = x, y, $z - 1$; #3 = $-x + 1$, $-y + 1$, $-z + 1$). (b) ORTEP view of coordination environment of Nd(III) in **2** along with the atom numbering scheme and thermal ellipsoids drawn at 45% probability (#1 = x, $-y + 1/2$, $z - 1/2$; #2 = $-x + 1$, $y - 1/2$, $-z + 1/2$; #3 = $-x + 1$, $y + 1/2$, $-z + 1/2$). (c) The coordination mode of H_3chhc^{3-} in **1** and **2**.

Table 2. The selected bond distances (Å) and hydrogen bonds (Å/°) for **1** and **2**.

1					
Pr–O(1)	2.431(7)	Pr–O(9)$^{\#3}$	2.544(8)	Pr–O(14)	2.553(9)
Pr–O(2)$^{\#1}$	2.420(8)	Pr–O(10)$^{\#3}$	2.619(8)	Pr–O(15)	2.485(8)
Pr–O(6)$^{\#2}$	2.379(8)	Pr–O(13)	2.650(9)	Pr–O(16)	2.475(9)
Hydrogen bonds in **1**					
D–H···A	∠DHA		D(D···A)		
O4–H4B···O5	172		2.566		
O8–H8B···O9	169		2.617		
O12–H12A···O1	164		2.723		
O13–H13C···O5$^{\#1}$	166		2.943		
O13–H13D···O6$^{\#1}$	132		2.771		
2					
Nd–O(1)	2.546(4)	Nd–O(6)$^{\#2}$	2.430(4)	Nd–O(14)	2.457(4)
Nd–O(2)	2.535(4)	Nd–O(10)$^{\#3}$	2.335(4)	Nd–O(15)	2.481(5)
Nd–O(5)$^{\#1}$	2.361(4)	Nd–O(13)	2.432(5)		
Hydrogen bonds in **2**					
D–H···A	∠DHA		D(D···A)		
O3–H3B···O6	164		2.738		
O8–H8A···O9	173		2.561		
O12–H12A···O1	164		2.607		

Symmetry transformations are shown in figure 1(a) and (b).

Pr(III) adopts nine-coordinate geometry, with five oxygens [O(1), O(2)$^{\#1}$, O(6)$^{\#2}$, O(9)$^{\#3}$, and O(10)$^{\#3}$; Pr–O distances 2.431(8)–2.619(8) Å] from four different H_3chhc^{3-}, three oxygens from three DMF molecules [O(14), O(15), and O(16); Pr–O distances 2.475(8)–2.553 (8) Å], and one coordinated water [O(13), Pr–O distance 2.650(8) Å] (table 2). The nine-coordinate praseodymium geometry is distorted monocapped square antiprism, in which the O(13) is located at the capping position and the O(1), O(9)$^{\#3}$, O(10)$^{\#3}$, O(15) and O(2)$^{\#1}$, O (6)$^{\#2}$, O14, O16 are defined in two square faces. The coordination environment of Pr is similar to $Pr_2(dpdc)_2(tpy)_2(NO_3)_2(H_2O)_2$ [27]. The asymmetric unit of **2** consists of one Nd (III), one H_3chhc^{3-}, and three DMF molecules [figure 1(b)], which has crystallized in the *P2₁/c* space group. The presence of coordinated water in **1** resulted in changes of space group and lattice parameters, compared with **2**. In **2**, each Nd(III) is eight-coordinated in a dicapped trigonal prismatic polyhedron, with five oxygens from different H_3chhc^{3-} anions [O(1), O(2), O(5)$^{\#1}$, O(6)$^{\#2}$, and O(10)$^{\#3}$; Nd–O distances 2.335(4)–2.516(4) Å] and three DMF ligands [O(13), O(14), and O(15); Nd–O distances 2.432(4)–2.481(4) Å], similar to the Nd(III) complex [28]. As expected, the *all-cis* configuration of H_6chhc is retained in both **1** and **2**. The H_3chhc^{3-} anions assume a *cis-e,a,e,a,e,a*-conformation with the central ring in chair-shaped configuration. Three carboxylates are in equatorial positions and three carboxylic groups in axial positions. Such configuration of H_3chhc^{3-} has been reported [17, 18]. At the same time, the H_3chhc^{3-} in both compounds adopt η^5,μ_4-coordination [figure 1(c)], in which one carboxylate chelates one Ln(III), the second is bidentate and bridges between Ln(III) ions, and the third is monodentate to one Ln(III). The bidentate carboxylate bridges the two symmetry-related Pr(III) ions to form dinuclear units with Pr···Pr distance 5.654 Å (Nd···Nd distance 5.734 Å in **2**). In both **1** and **2**, three hydroxyl oxygens of the carboxylic acid groups as donors form intra-ligand hydrogen bonds (table 2) with three oxygens from three carboxylate groups, further stabilizing the *cis* conformation. While the coordinated water molecules in **1** donate two hydrogens to form inter-ligand hydrogen bonds with two carboxylate oxygens.

In **1**, Pr(III) centers are interconnected by the η^5,μ_4-H_3chhc^{3-} anions, resulting in 2-D metal–organic layers [figure 2(a)], which extend infinitely parallel to (1 0 0). The uncoordinated axial carboxylic groups point on either side of the layers. The crystal structures adopt

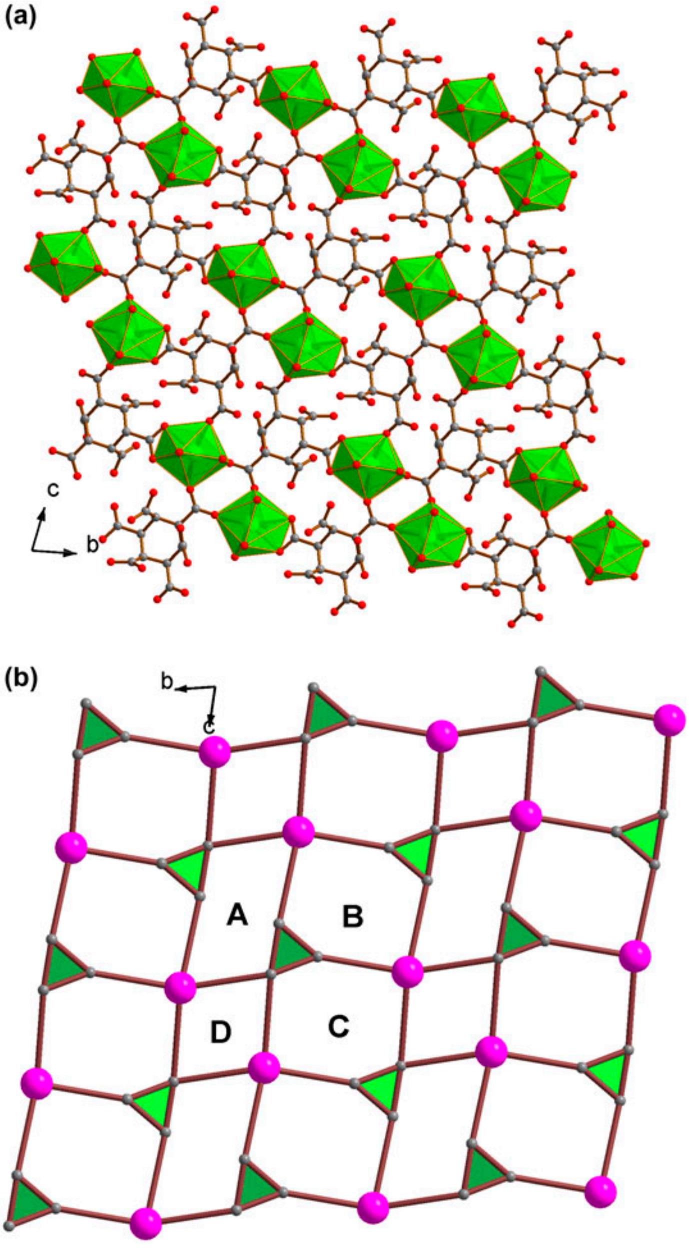

Figure 2. (a) View of $[4^4, 6^2]$ 2-D structure of **1**. (b) The topology of the 2-D layer (the red balls and green triangles standing for $[Pr(DMF)_3(H_2O)]^{3+}$ ions and H_3chhc^{3-} anions, respectively; the coordinated DMF molecules and hydrogens are deleted for clarity) (see http://dx.doi.org/10.1080/00958972.2015.1023717 for color version).

2-D (4,4)-rectangular networks [(4^4, 6^2) in extended Schläfli notation] growing in the *bc* plane [figure 2(b)]. In the network, the $[Pr(DMF)_3(H_2O)]^{3+}$ complex ions [red balls in figure 2(b)] are four-fold nodes and the H_3chhc^{3-} anions are considered as four-fold connectors [green triangles in figure 2(b)]. The topological structure of **2** is similar to **1**, though one coordinated water has been decreased. In the lanthanide–H_3chhc^{3-} coordination polymers with (4^4, 6^2) 2-D networks, the eight-coordinate central Ln(III) ions in **2** are found. In the 2-D network of **1**, four kinds of macrocycles were produced by bridging of H_3chhc^{3-} ligands, and their sizes are 9.588 × 7.100 Å (A), 7.105 × 5.654 Å (B), 8.177 × 8.453 Å (C), 8.677 × 8.066 Å (D), respectively [9.398 × 6.826 Å (A), 7.147 × 5.734 Å (B), 8.387 × 8.084 Å (C and D) in **2**].

The coordination modes of H_3chhc^{3-} in lanthanide compounds are shown in scheme 2 [(a) $\eta^6\mu_3$) and (b) $\eta^5\mu_4$]. In $Eu(H_3chhc)(H_2O)\cdot 3H_2O$ [17] and $Gd(H_3chhc)(H_2O)\cdot 3H_2O$ [18], three carboxylate groups adopt $\eta^6\mu_3$ coordination chelating a metal ion to form a 2-D 6^3 (extended Schläfli notation) network (scheme 2), in which both metal ions and H_3chhc^{3-} anions are trigonal nodes. These compounds crystallize in chiral space group *P2₁*. However, the coordination mode η^5,μ_4- of H_3chhc^{3-} is found in $Eu(H_3chhc)(H_2O)\cdot 6H_2O$ [17], Gd $(H_3chhc)(H_2O)\cdot 6H_2O$ [18], **1** and **2**, which crystallize in centrosymmetric space groups *P2₁/n* (the previous two compounds), *P-1* (**1**), and *P2₁/c* (**2**). The crystal structures of these compounds are 2-D (4,4)-rectangular networks [(4^4, 6^2) nets in extended Schläfli notation]. Though these compounds have similar compositions, their topological structures and space groups are different due to changes of coordination modes of three carboxylate groups in the H_3chhc^{3-} anions.

The polycarboxylate ligands in reported lanthanide coordination polymers [29–33] are mainly benzene-based polycarboxylates. Compared with the benzene-based polycarboxylates, H_6chhc with six-membered ring and single-bonded cyclo skeleton can undergo isomerization during lanthanide complexation by transforming equatorial or axial orientations of the six carboxyl groups. The deprotonation degree of six carboxyl groups in H_6chhc can also affect the topology and dimensionality of lanthanide coordination polymers. Therefore, the H_6chhc can be expected to synthesize more lanthanide coordination polymers with interesting structures.

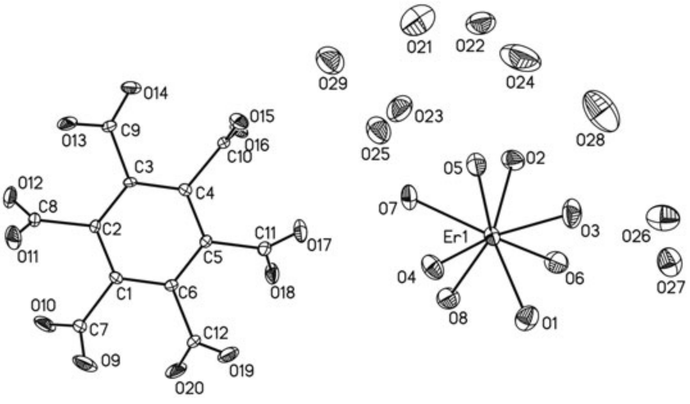

Figure 3. ORTEP view of coordination environment of Er(III) in **3** along with the atom numbering scheme and thermal ellipsoids drawn at 45% probability.

3.2. *The crystal structures $Er(H_2O)_8{\cdot}(H_3Mel){\cdot}9(H_2O)$ (3) and $[Yb(H_2O)_8]{\cdot}(H_3Mel){\cdot}8.5(H_2O)$ (4)*

Crystallographic analysis revealed that **3** and **4** are isostructural. Hence, only **3** will be discussed as a representative. The asymmetric unit of **3** comprises one Er(III), eight coordinated waters, one H_3Mel^{3-} anion, and nine lattice waters (figure 3). Each Er(III) has a dodecahedral coordination environment with eight oxygens from water. The Er–O bond distances are not equal (table 3). Therefore, the coordination polyhedron of Er(III) is not a regular dodecahedron. The H_3Mel^{3-} anions do not coordinate with Er(III) ion, but are counter ions of $Er(H_2O)_8^{3+}$. Although H_3Mel^{3-} has similar structure with H_3chhc^{3-}, they are not coordinated to Er(III) ions at room temperature in aqueous solution. As the coordinated carboxylate groups of fully deprotonated mellitate anions in lanthanide complexes display chelating and bridging coordination modes, these lanthanide–mellitate complexes

Table 3. The selected bond distances (Å) and hydrogen bonds (Å/°) for **3** and **4**.

3					
Er–O(1)	2.371(3)	Er–O(4)	2.304(3)	Er–O(7)	2.392(2)
Er–O(2)	2.338(3)	Er–O(5)	2.349(2)	Er–O(8)	2.318(3)
Er–O(3)	2.331(3)	Er–O(6)	2.376(3)		
Hydrogen bonds in **3**					
D–H···A	∠DHA	D(D···A)	D–H···A	∠DHA	D(D···A)
O1···H1A···O15$^{\#1}$	176	2.882	O1···H1B···O22$^{\#2}$	168	2.810
O2···H2A···O24	171	2.807	O2···H2B···O12$^{\#3}$	168	2.697
O3···H3A···O28	173	2.671	O3···H3B···O27	160	2.738
O4···H4A···O17$^{\#1}$	172	2.761	O4···H4B···O25$^{\#1}$	169	2.631
O5···H5A···O25	159	2.710	O5···H5B···O19$^{\#1}$	156	2.779
O6···H6B···O26	163	2.882	O7···H7A···O14$^{\#3}$	156	2.778
O7···H7B···O17	160	2.834	O8···H8A···O16$^{\#3}$	154	2.677
O10···H10···O12$^{\#4}$	177	2.515	O13···H13···O20$^{\#5}$	174	2.511
O18···H18···O16$^{\#3}$	167	2.519	O22···H22A···O19$^{\#1}$	174	2.864
O22···H22B···O27$^{\#5}$	167	2.796	O23···H23A···O15$^{\#6}$	162	2.808
O23···H23B···O19$^{\#1}$	143	2.997	O24···H24A···O11$^{\#7}$	120	2.781
O25···H25B···O23	173	2.648	O26···H26A···O9$^{\#7}$	166	2.924
O27···H27A···O26	144	2.786	O27···H27B···O11$^{\#1}$	172	2.794
O28···H28A···O24	121	2.805	O28···H28B···O9$^{\#1}$	155	2.751
4					
Yb–O(1)	2.361(3)	Yb–O(4)	2.292(3)	Yb–O(7)	2.366(3)
Yb–O(2)	2.323(3)	Yb–O(5)	2.336(3)	Yb–O(8)	2.312(3)
Yb–O(3)	2.310(3)	Yb–O(6)	2.371(3)		
Hydrogen bonds in **4**					
D–H···A	∠DHA	D(D···A)	D–H···A	∠DHA	D(D···A)
O1···H1A···O15$^{\#1}$	154	2.877	O1···H1B···O22$^{\#2}$	167	2.806
O2···H2A···O24	176	2.812	O2···H2B···O12$^{\#3}$	157	2.719
O3···H3A···O28	173	2.673	O3···H3B···O27	164	2.759
O4···H4A···O17$^{\#1}$	176	2.770	O4···H4B···O25$^{\#1}$	169	2.652
O5···H5A···O25	157	2.734	O5···H5B···O19$^{\#1}$	156	2.799
O6···H6B···O26	174	2.881	O7···H7A···O14$^{\#3}$	160	2.800
O7···H7B···O17	162	2.826	O8···H8A···O16$^{\#3}$	136	2.888
O10···H10···O12$^{\#4}$	171	2.511	O13···H13···O20$^{\#5}$	167	2.509
O18···H18···O16$^{\#3}$	171	2.515	O22···H22A···O19$^{\#1}$	172	2.870
O22···H22B···O27$^{\#5}$	165	2.825	O23···H23A···O15$^{\#6}$	165	2.810
O23···H23B···O19$^{\#1}$	138	2.985	O24···H24A···O11$^{\#7}$	111	2.832
O25···H25B···O23	168	2.677	O26···H26A···O9$^{\#7}$	171	2.934
O27···H27A···O26	161	2.792	O27···H27B···O11$^{\#1}$	168	2.812
O28···H28A···O24	116	2.957	O28···H28B···O9$^{\#1}$	159	2.809

Symmetry codes: #1 = $-x+1$, $-y+1$, $-z+1$; #2 = x, $y+1$, z; #3 = $-x+1$, $y+1/2$, $-z+1/2$, #4 = $-x+2$, $y+1/2$, $-z+1/2$; #5 = x, $y-1$, z; #6 = $-x+1$, $-y$, $-z+1$; #7 = $x-1$, y, z.

can be divided into two categories, one category was formed under hydrothermal method [12, 16] and another was crystallized at room temperature [24–26]. The hydrothermal synthesized products $[Ln_2(Mel)(H_2O)_x]_n$ have lower levels of ancillary aquation ($x = 4–6$) compared with the analogs ($x = 8–10$) prepared at room temperature. This phenomenon also explains the formation of **3** and **4**.

In H_3Mel^{3-}, three hydroxyl oxygens (O(10), O(13), and O(18)) of the carboxylic groups are hydrogen bond donors to O(12), O(16), and O(20) from three carboxylate groups of adjacent H_3Mel^{3-} anions (table 3). These hydrogen bond distances (D···A) are shorter than other hydrogen bonds in the crystal structure of **3**. By these hydrogen bonds, the H_3Mel^{3-} anions are interconnected to form 2-D organic supramolecular layers perpendicular to the (0 0 1) direction [figure 4(a)]. The $Er(H_2O)_8^{3+}$ ions are sandwiched between the 2-D organic

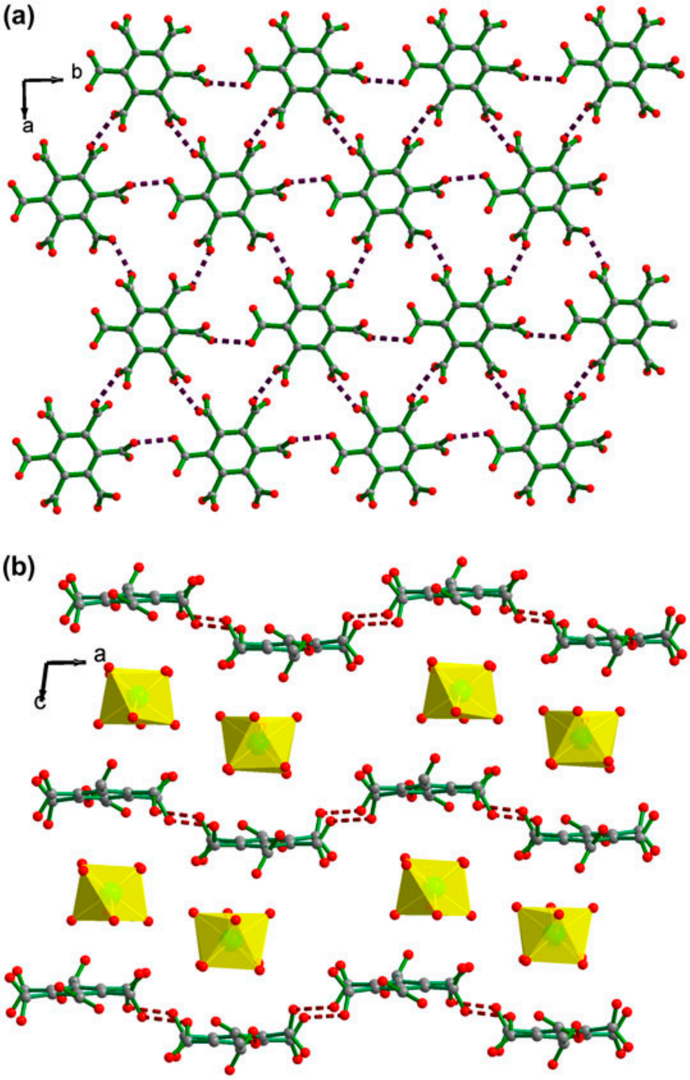

Figure 4. (a) The 2-D supramolecular layer in **3**. (b) The inorganic and organic layers alternating structure in **3**.

supramolecular layers [figure 4(b)] and organic and inorganic alternating layer structures are obtained. Lattice water molecules exist in these layers. Substantial hydrogen bonds exist between coordinated water molecules, lattice water molecules, and carboxylates.

3.3. *Luminescence properties*

The emission spectra of solid state **1** and **2** were recorded at room temperature under excitation wavelengths of 286 and 283 nm, respectively, and the results are shown in figure 5(a). Broad emission bands centered at 345 nm for **1** and 340 and 369 nm for **2** are ascribed to the π–π* electronic transition of the H_3chhc^{3-} [34]. The different emission bands between **1** and **2** indicate that the different lanthanide ions and coordination environments affect the

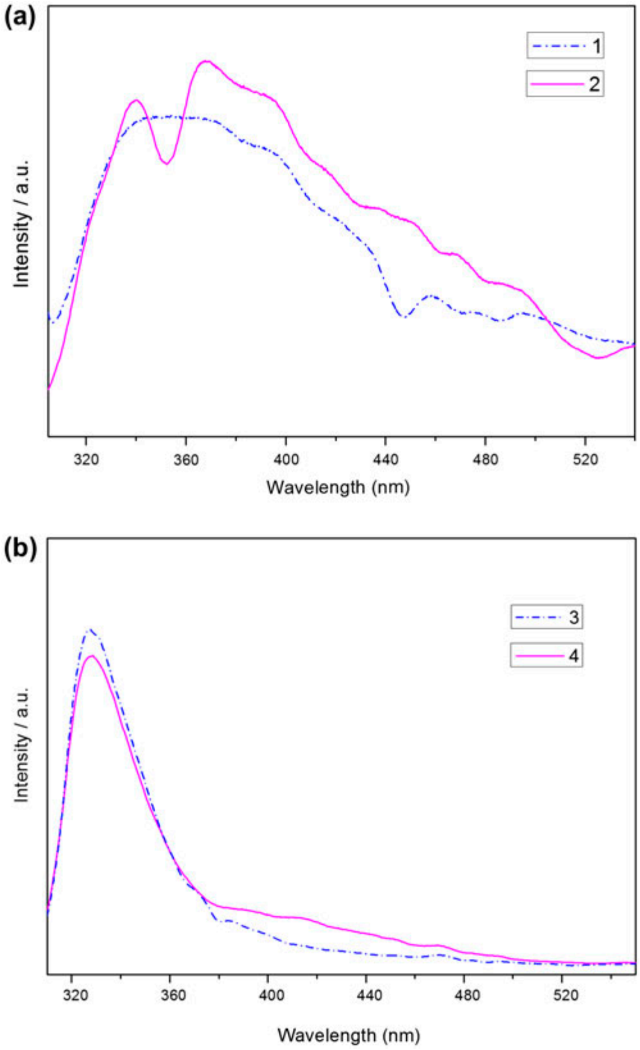

Figure 5. The solid-state luminescence emission spectra of (a) **1**, **2** and (b) **3**, **4**.

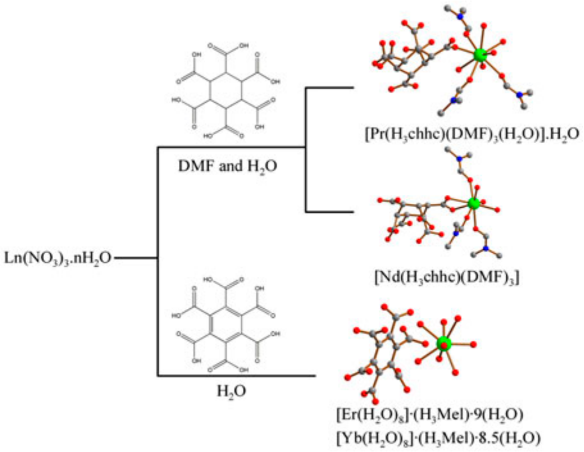

Scheme 1. The lanthanide complexes based on two hexacarboxylic acids.

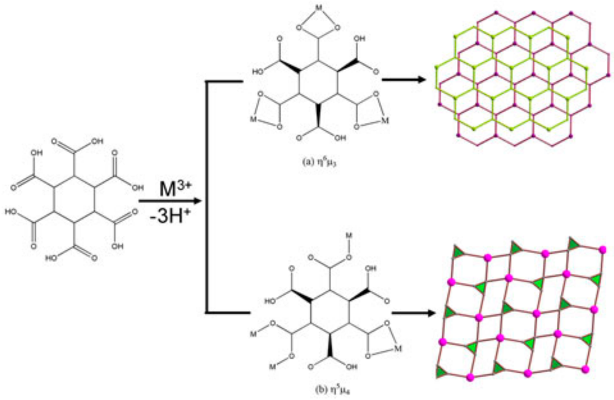

Scheme 2. The relation between the coordination modes of H3chhc^{3-} and topological structures.

energy absorption of the complexes by coordination interaction between lanthanide and H_3chhc^{3-} anions. As shown in the emission spectra in figure 5(b), **3** and **4** have the same emission band located at 327 nm under an excitation at 275 nm, which can be assigned to the π–π* transitions of the H_3Mel^{3-} [27]. Unlike H_3chhc^{3-} in **1** and **2**, the H_3Mel^{3-} anions were not coordinated to lanthanide ions, hence the different lanthanide ions did not affect the energy transfer, resulting in both **3** and **4** having the same emission bands.

3.4. *Powder X-ray diffraction (PXRD)*

The isolated samples of **1–4** were characterized by powder X-ray diffraction (PXRD) at room temperature. The PXRD and the simulated XRD patterns of **1–4** from single-crystal X-ray data are shown in figure S1 (see online supplemental material at http://dx.doi.org/10.1080/00958972.2015.1023717). The PXRD pattern of **2** is in agreement with the simulated

XRD patterns, indicating a single phase is prepared. The differences between the simulated and experimental XRD patterns of **1**, **3**, and **4** may be due to water lost during the grinding process, which could lead to change of structures.

4. Conclusion

Four lanthanide complexes with H_3chhc^{3-} or H_3Mel^{3-} have been synthesized at room temperature without adjusting pH of solution. In **1** and **2**, H_3chhc^{3-} have a *cis-e,a,e,a,e,a*-conformation with the central ring in chair configuration, three carboxylate groups are in the equatorial position and three carboxylic groups are in the axial position. The crystal structures of **1** and **2** are assembled into a 2-D (4,4)-rectangular network by three coordination sites of $\eta^5\mu_4$ H_3chhc^{3-} anions in equatorial positions. In lanthanide–H_3chhc^{3-} coordination polymers with (4^4, 6^2) 2-D network, the eight-coordinate Ln(III) ions are found. The deprotonation degree of six carboxyl groups in H_6chhc can affect the topology and dimensionality of lanthanide coordination polymers.

Although the H_3Mel^{3-} in **3** and **4** have similar structure with H_3chhc^{3-} anions, they are not coordinated to Ln(III). The tri-protonated form (H_3Mel^{3-}) of mellitic acid has not been found in complexes. In **3** and **4**, the H_3Mel^{3-} interconnects to form 2-D organic supramolecular layers by hydrogen bonds between the oxygens from three carboxylic and carboxylate groups. The $\mathrm{Ln(H_2O)}_8^{3+}$ complex ions are sandwiched between the 2-D organic supramolecular layers, and organic and inorganic alternating layer structures are obtained. Hydrothermal synthesized products of lanthanide with mellitic acid have lower levels of ancillary aquation compared with the analogs prepared at room temperature. In the future, more lanthanide coordination polymers with novel structures can be synthesized based on hexacarboxylic acids.

Supplementary material

Complete crystallographic data for the structures reported in this paper have been deposited in the CIF format with the Cambridge Crystallographic Data Center as supplementary publication nos. CCDC 991029, 991030, 991031 and 991032. Copies of the data can be obtained free of charge on application to CCDC, 12 Union Road, Cambridge CB2 1EZ, UK (Fax: (44) 1223336033; E-mail: deposit@ccdc.cam.ac.uk).

Funding

This work was supported by the National Basic Research Program of China [grant number 2010CB732300]; Foundation of Zhejiang Province Education Commission of China [grant number Y201224213]; the Subject Object of Ningbo University [grant number xkl141029].

References

[1] B.H. Ye, M.L. Tong, X.M. Chen. *Coord. Chem. Rev.*, **249**, 545 (2005).
[2] K.A. White, S. Petoud, N.L. Rose. *Chem. Commun.*, 4506 (2009).
[3] J. Rocha, L.D. Carlos, F.A. Almeida Paz, D. Ananias. *Chem. Soc. Rev.*, **40**, 926 (2011).

[4] P. Wang, J.P. Ma, Y.B. Dong, R.Q. Huang. *J. Am. Chem. Soc.*, **129**, 10620 (2007).
[5] Y.F. Han, X.Y. Li, L.Q. Li, C.L. Ma, Z. Shen, Y. Song, X.Z. You. *Inorg. Chem.*, **49**, 10781 (2010).
[6] M.B. Zhang, J. Zhang, S.T. Zheng, G.Y. Yang. *Angew. Chem. Int. Ed.*, **44**, 1385 (2005).
[7] J.W. Cheng, J. Zhang, S.T. Zheng, M.B. Zhang, G.Y. Yang. *Angew. Chem. Int. Ed.*, **45**, 73 (2006).
[8] E. Shyu, R.M. Supkowski, R.L. LaDuca. *Inorg. Chem.*, **48**, 2723 (2009).
[9] K.M.L. Taylor, A. Jin, W.B. Lin. *Angew. Chem. Int. Ed.*, **47**, 7722 (2008).
[10] J. Wang, Y.C. Ou, Y. Shen, L. Yun, J.D. Leng, Z.J. Lin, M.L. Tong. *Cryst. Growth Des.*, **9**, 2442 (2009).
[11] L. Pan, E.B. Woodlock, X.T. Wang, C. Zheng. *Inorg. Chem.*, **39**, 4174 (2004).
[12] S.S.Y. Chui, A. Siu, X. Feng, Z.Y. Zhang, T.C.W. Mak, I.D. Williams. *Inorg. Chem. Commun.*, **4**, 467 (2001).
[13] Z.J. Lin, M.L. Tong. *Coord. Chem. Rev.*, **255**, 421 (2011).
[14] Y.F. Han, L. Fu, L. Mafra, F.N. Shi. *J. Solid State Chem.*, **186**, 165 (2012).
[15] J. Wang, M. Xu, T.T. Su. *Chin. J. Inorg. Chem.*, **27**, 737 (2011).
[16] X.Y. Tang, S.T. Yue, P. Li, N. Wang, Y.L. Liu. *J. Rare Earths*, **26**, 800 (2008).
[17] P. Thuéry, B. Masci. *Cryst. Growth Des.*, **10**, 3626 (2010).
[18] L. Cañadillas-Delgado, O. Fabelo, J. Pasán, M. Julve, F. Lloret, C. Ruiz-Pérez. *Polyhedron*, **29**, 188 (2010).
[19] J. Wang, Y.H. Zheng, M.L. Tong. *Chem. Commun.*, 3166 (2006).
[20] J. Wang, L.L. Zheng, C.J. Li, Y.Z. Zheng, M.L. Tong. *Cryst. Growth Des.*, **6**, 357 (2006).
[21] J. Wang, S. Hu, M.L. Tong. *Eur. J. Inorg. Chem.*, 2069 (2006).
[22] G.M. Sheldrick. *SHELXS-97, program zur Lösung von Kristallstrukturen*, University of Göttingen, Göttingen (1997).
[23] G.M. Sheldrick. *SHELXL-97, program zur Lösung von Kristallstrukturen*, University of Göttingen, Göttingen (1997).
[24] L.P. Wu, M. Munakata, T. Kuroda-Sowa, M. Maekawa, Y. Suenaga. *Inorg. Chim. Acta*, **249**, 183 (1996).
[25] L.P. Wu. *J. Coord. Chem.*, **37**, 361 (1996).
[26] C. Robl, S. Hentschel. *Z. Naturforsch. Teil B*, **47**, 1561 (1992).
[27] H.Z. Xie, G.Z. Lu. *J. Rare Earths*, **31**, 639 (2013).
[28] L.F. Zhao, Y.S. Chen. *Acta Chim. Sinica*, **65**, 667 (2007).
[29] I.U. Khan, S. Sharif, O. Sahin. *J. Coord. Chem.*, **66**, 3113 (2013).
[30] Z.J. Xiahou, Y.L. Wang, Q.Y. Liu, L.Q. Li, L.J. Zhou. *J. Coord. Chem.*, **66**, 2910 (2013).
[31] F. Zhang, X.T. Huang, Y.Y. Tian, Y.X. Gong, X.Y. Chen, J.J. Lin, D.S. Lu, Y.L. Zhang, R.H. Zeng, S.R. Zheng. *J. Coord. Chem.*, **66**, 2659 (2013).
[32] L. Cheng, Q.N. Cao, X.Y. Zhang, S.H. Gou, L. Fang. *J. Coord. Chem.*, **66**, 481 (2013).
[33] H.Z. Xie, G.Z. Lu. *J. Lumin.*, **145**, 119 (2014).
[34] J. Zhu, H.F. Song, J.W. Sun, P.F. Yan, G.F. Hou, G.M. Li. *Synth. Met.*, **192**, 29 (2014).